

# EFFICIENT UNCERTAINTY QUANTIFICATION FOR BIOTRANSPORT IN TUMORS WITH UNCERTAIN MATERIAL PROPERTIES

**Alen Alexanderian**

Department of Mathematics  
Center for Research in Scientific Computation  
North Carolina State University  
Raleigh, NC 27695  
Email: alexanderian@ncsu.edu

**William Reese**

Department of Mathematics  
North Carolina State University  
Raleigh, NC 27695

**Ralph C. Smith**

Department of Mathematics  
Center for Research in Scientific Computation  
North Carolina State University  
Raleigh, NC 27695

**Meilin Yu\***

Department of Mechanical Engineering  
University of Maryland, Baltimore County  
Baltimore, MD 21250  
Email: mlyu@umbc.edu

*sure field in a low-dimensional parameter space is constructed using the truncated KL expansion technique.*

## ABSTRACT

We consider modeling of single phase fluid flow in heterogeneous porous media governed by elliptic partial differential equations (PDEs) with random field coefficients. Our target application is biotransport in tumors with uncertain heterogeneous material properties. We numerically explore dimension reduction of the input parameter and model output. In the present work, the permeability field is modeled as a log-Gaussian random field, and its covariance function is specified. Uncertainties in permeability are then propagated into the pressure field through the elliptic PDE governing porous media flow. The covariance matrix of pressure is constructed via Monte Carlo sampling. The truncated Karhunen–Loève (KL) expansion technique is used to decompose the log-permeability field, as well as the random pressure field resulting from random permeability. We find that although very high-dimensional representation is needed to recover the permeability field when the correlation length is small, the pressure field is not sensitive to high-order KL terms of input parameter, and itself can be modeled using a low-dimensional model. Thus a low-rank representation of the pres-

## INTRODUCTION

Understanding biotransport processes in tumors with uncertain material properties is important for agent (e.g., drug, nanoparticles) delivery in cancer treatment [1, 2]. Biotransport processes in tumors can be modeled as flows in porous media, with random heterogeneous material properties, governed by different types of PDEs: an elliptic PDE, which describes the pressure distribution; and a hyperbolic PDE, which describes agent delivery in porous media [3]. Therefore, uncertainties in the PDE coefficient fields will be propagated into the flow field via complex fluid and tumor structure interaction described by these PDEs [4]. In this work, we focus on elliptic PDEs, modeling single phase fluid flow in heterogeneous porous media. The permeability field is modeled as a log-Gaussian random field, and the goal is to efficiently simulate the uncertain pressure field. The random permeability field is represented through its KL expansion [5].

The idea of using KL expansions for representing random field coefficients in PDEs has been a common modeling approach for many years; see e.g., [6–15]. Typically, the random field coefficient is represented using a truncated KL expansion

---

\*Address all correspondence to this author.

August 7, 2018

with enough terms to ensure a sufficiently accurate representation. This truncated KL expansion, which is computed upfront, is then substituted in the governing PDEs, after which appropriate uncertainty analysis is performed. The study presented herein takes a different point of view: instead of relying on a truncated KL expansion of the parameter, computed a priori and independently of the governing PDE, we argue that only the KL terms that the PDE solution operator is sensitive to should be retained. Moreover, we explore the KL expansion of the PDE solution, for computing a low-rank representation of the model output.

In presence of small correlation lengths, a large number of terms in the KL expansion are required to represent the uncertain permeability field. However, it is observed that, for the pressure equation, the PDE solution operator is not sensitive to the high-order KL terms of the parameter. This enables reducing the dimension of the input parameter, by focusing on the KL terms that are most influential to variations in the pressure field. The PDE solution—the pressure field—itself can also be represented via a truncated KL expansion. It is again observed that a low-rank representation of the pressure field is often afforded by a suitably truncated KL expansion. Combining these ideas enables a low-rank representation of the pressure field in a low-dimensional parameter space. We first illustrate these ideas using a one-dimensional (1D) model elliptic PDE, and then further explore the proposed approach in a two-dimensional (2D) model of biotransport in a tumor with uncertain material properties.

## BACKGROUND ON RANDOM FIELDS

We let  $(\Omega, \mathcal{F}, P)$  be a probability space, where  $\Omega$  is a sample space,  $\mathcal{F}$  is an appropriate  $\sigma$ -algebra, and  $P$  is a probability measure. Let  $D \subset \mathbb{R}^d$ , with  $d = 1, 2$ , or  $3$ , be a  $d$ -dimensional bounded physical domain. We consider stochastic processes of form  $Z : D \times \Omega \rightarrow \mathbb{R}$ ; for background material on stochastic processes, we refer the reader to [16]. From a practical point of view,  $Z(\mathbf{x}, \omega)$  can be used to model uncertain field parameters appearing in PDEs governing the physical systems.

We call a stochastic process *centered* if  $E[Z(\mathbf{x}, \cdot)] = 0$  for all  $\mathbf{x} \in D$ , where  $E[\cdot]$  denotes mathematical expectation, i.e.,  $E[Z(\mathbf{x}, \cdot)] = \int_{\Omega} Z(\mathbf{x}, \omega) P(d\omega)$ . A process  $Z$  is said to be *mean square continuous* if for all  $\mathbf{x} \in D$ ,

$$\lim_{\mathbf{h} \rightarrow \mathbf{0}} E[(Z(\mathbf{x} + \mathbf{h}, \cdot) - Z(\mathbf{x}, \cdot))^2] = 0.$$

**Karhunen–Loève expansion.** The covariance function  $c : D \times D \rightarrow \mathbb{R}$  of a stochastic process  $Z$  is defined as

$$c(\mathbf{x}, \mathbf{y}) = E[Z(\mathbf{x}, \cdot)Z(\mathbf{y}, \cdot)] - E[Z(\mathbf{x}, \cdot)]E[Z(\mathbf{y}, \cdot)], \quad (1)$$

and the corresponding correlation function is given by,

$$\rho(\mathbf{x}, \mathbf{y}) = \frac{c(\mathbf{x}, \mathbf{y})}{\sqrt{c(\mathbf{x}, \mathbf{x})}\sqrt{c(\mathbf{y}, \mathbf{y})}}.$$

Given the covariance function of  $Z(\mathbf{x}, \omega)$ , the associated *covariance operator*  $C : L^2(D) \rightarrow L^2(D)$  is defined as

$$[Cu](\mathbf{x}) = \int_D c(\mathbf{x}, \mathbf{y})u(\mathbf{y})d\mathbf{y}, \quad (2)$$

where  $L^2(D) = \{f : D \rightarrow \mathbb{R} : \int_D |f(\mathbf{x})|^2 d\mathbf{x} < \infty\}$ .

Let  $Z : D \times \Omega \rightarrow \mathbb{R}$  be a centered mean-square continuous stochastic process, and let  $\{e_i\}_{i=1}^{\infty}$  be the orthonormal basis of eigenvectors of the covariance operator  $C$  of  $Z(\mathbf{x}, \omega)$  with corresponding (non-negative) eigenvalues  $\{\lambda_i\}_{i=1}^{\infty}$ :

$$\int_D c(\cdot, \mathbf{y})e_i(\mathbf{y})d\mathbf{y} = \lambda_i e_i(\cdot), \quad i = 1, 2, \dots \quad (3)$$

The process  $Z(\mathbf{x}, \omega)$  can be represented as

$$Z(\mathbf{x}, \omega) = \sum_{i=1}^{\infty} \sqrt{\lambda_i} \xi_i(\omega) e_i(\mathbf{x}), \quad (4)$$

where  $\xi_i$  are centered mutually uncorrelated random variables with unit variance and are given by,

$$\xi_i(\omega) = \frac{1}{\sqrt{\lambda_i}} \int_D Z(\mathbf{x}, \omega) e_i(\mathbf{x}) d\mathbf{x}.$$

The convergence of the series (4) is uniform in  $D$ , and is mean square in  $\Omega$  [5]. The series expansion (4) is known as the KL expansion [5, 17–19] of  $Z(\mathbf{x}, \omega)$ .

**Numerical computation of KL expansion.** Here we outline a basic approach for computing the KL expansion of a stochastic process (random field). To numerically compute the KL expansion of a stochastic process we need to first solve the eigenvalue problem (3). Here, we follow Nyström’s approach [20], in which the generalized eigenvalue problem is discretized via quadrature. In some cases, one can specify the covariance function of the process via an analytic formula. This is the case, for instance, when modeling uncertain coefficient fields in mathematical models via Gaussian processes, as seen later in the present work. On the other hand, in some cases, we only can simulate realizations of a given stochastic process. The latter is the case, when working with solution of a PDE with uncertain parameters. Let  $U$  denote the solution of such a PDE. In practice,

often one parameterizes model uncertainties via a random vector  $\boldsymbol{\xi}(\omega)$ , in which case the random field solution  $U = U(\mathbf{x}, \boldsymbol{\xi})$  of the PDE can be computed for specific realizations of  $\boldsymbol{\xi}$ . To compute the truncated KL expansion,

$$\begin{aligned} U(\mathbf{x}, \boldsymbol{\xi}) &\approx \bar{U}(\mathbf{x}) + \sum_{i=1}^{N_{kl}} \sqrt{\lambda_i} u_i(\boldsymbol{\xi}) e_i(\mathbf{x}), \\ \bar{U}(\mathbf{x}) &= E[U(\mathbf{x}, \cdot)], \\ u_i(\boldsymbol{\xi}) &= \frac{1}{\sqrt{\lambda_i}} \int_D (U(\mathbf{x}, \boldsymbol{\xi}) - \bar{U}(\mathbf{x})) e_i(\mathbf{x}) d\mathbf{x}, \end{aligned} \quad (5)$$

the covariance function of the process needs to be approximated via sampling; this in turn leads to an approximate covariance operator  $C$  for the process. The approximate covariance operator is then used to formulate and solve the generalized eigenvalue problem to find (approximations to)  $\lambda_i$  and  $e_i$ ,  $i = 1, \dots, N_{kl}$ . In Algorithm 1, we summarize the process of computing the truncated KL expansion of a random process  $U(\mathbf{x}, \boldsymbol{\xi})$  by sampling its covariance function. In the sequel, we call the coefficients  $u_i$  in (5) the *KL modes*. For further details on numerical techniques for computing KL expansions, we refer to [21].

## MODEL 1D ELLIPTIC EQUATION WITH RANDOM COEFFICIENT FUNCTION

Let  $(\Omega, \mathcal{F}, P)$  be a probability space. We consider the following elliptic boundary value problem: for  $\omega \in \Omega$ , find a function  $p$  such that

$$\begin{aligned} -\frac{d}{dx} \left( \kappa(x, \omega) \frac{dp(x, \omega)}{dx} \right) &= f(x), \quad x \in D = (-1, 1), \\ p(-1, \omega) &= 1, \\ p(1, \omega) &= 0. \end{aligned} \quad (6)$$

In the following numerical experiments, the right hand side function is given by  $f(x) = \cos(\pi x) + \sin(2\pi x)$ . We model the coefficient function  $\kappa(x, \omega)$  as a log-Gaussian random field in the following manner. Let  $Z(x, \omega)$  be a centered Gaussian process with covariance function,

$$c_Z(x, y) = \exp \left\{ -\frac{|x - y|}{\ell} \right\}. \quad (7)$$

The number  $\ell \geq 0$  is the correlation length of the process, which in the present work is set to  $\ell = 1/4$ ; i.e., 12.5% of the length of the domain. We define  $\kappa(x, \omega) = \exp(a(x, \omega))$  with

$$a(x, \omega) = a_0(x) + \sigma Z(x, \omega). \quad (8)$$

Here  $\sigma^2$  is the pointwise variance and  $a_0$  is the pointwise mean; these parameters are chosen to obtain a pointwise mean of  $m = 0.1$  and pointwise standard deviation of  $s = .07$  for  $\kappa(x, \omega)$ : we let  $\sigma^2 = \log(1 + s^2/m^2)$  and  $a_0 \equiv \log(m/\sqrt{1 + s^2/m^2})$ .<sup>1</sup>

To facilitate computations, we consider a truncated KL expansion of  $Z(\mathbf{x}, \omega)$ ; thus, we use

$$a_{N_{kl}}^a(x, \omega) = a_0 + \sigma \sum_{i=1}^{N_{kl}} \sqrt{\lambda_i} \xi_i(\omega) e_i(x), \quad (9)$$

where  $(\lambda_i, e_i)$  are eigenpairs of the covariance operator of  $Z(x, \omega)$ . Due to Gaussianity of the process,  $\xi_i$  are independent standard normal random variables. The random vector

$$\boldsymbol{\xi} = [\xi_1 \ \xi_2 \ \dots \ \xi_{N_{kl}}]^T \quad (10)$$

completely characterizes the uncertainty in the PDE (6), and its solution  $p(x, \omega) = p(x, \boldsymbol{\xi}(\omega))$ .

The eigenpairs of the covariance operator  $[C_Z u](x) = \int_D c_Z(x, y) u(y) dy$  are computed numerically by discretizing the corresponding generalized eigenvalue problem, as explained in the previous section. The truncation of the KL expansion of  $Z(x, \omega)$  is guided by considering the ratio,

$$r(N) = \frac{\sum_{i=1}^N \lambda_i}{\sum_{i=1}^{\infty} \lambda_i}, \quad (11)$$

which quantifies the percentage of the average variance captured by the first  $N$  KL terms.

**Realizations of  $a(x, \omega)$  and the corresponding realizations of  $p(x, \omega)$ .** Using the truncated KL expansion in (9), we can approximate the log-coefficient field efficiently. The top-left image in Figure 1 shows several realizations of  $a(x, \omega)$ , corresponding to  $N_{kl}^a = 70$ . The corresponding solutions of the problem (6) are reported in Figure 1 (bottom-left). To demonstrate the impact of changing the number of KL terms on the realizations of  $a(x, \omega)$ , we consider a fixed realization of  $a(x, \omega)$  as  $N_{kl}^a$  increases. We note in Figure 1 (top-right) that for the present process with the specific choice of correlation structure, sufficiently large  $N_{kl}^a$  is needed to capture the fluctuations of the random field reasonably well. On the other hand, the PDE solution seems insensitive to the higher-order KL terms of the parameter, as seen in Figure 1 (bottom-right). This suggests that it is possible to reduce parameter dimension by retaining only the terms in the KL expansion (9) that have notable impact on PDE solution.

<sup>1</sup>Here we use the well-known formulas relating the mean and variance of a log-normal random variable  $Y = \exp(a_0 + \sigma X)$ , where  $X$  is standard normal, to  $a_0$  and  $\sigma^2$  (the mean and variance of  $\log Y$ ).

---

**Algorithm 1** Computing KL expansion of a random process  $U(\mathbf{x}, \boldsymbol{\xi})$  using Nyström's approach.

---

**Input:** (i) A quadrature formula on  $D$  with nodes and weights  $\{\mathbf{x}_m, w_m\}_{m=1}^{N_{\text{quad}}}$ ; (ii) function evaluations  $\{U(\mathbf{x}_m, \boldsymbol{\xi}^k)\}$ ,  $m \in \{1, \dots, N_{\text{quad}}\}$ ,  $k \in \{1, \dots, N\}$ ; (iii) truncation level  $N_{kl}$ .

**Output:** Eigenpairs of the discretized covariance operator,  $\{(\lambda_i, \mathbf{e}_i)\}_{i=1}^{N_{kl}}$ , and KL modes  $\{u_i\}_{i=1}^{N_{kl}}$ .

1: Compute the mean

$$\bar{U}_m = \frac{1}{N} \sum_{j=1}^N U(\mathbf{x}_m, \boldsymbol{\xi}^j), \quad m \in \{1, \dots, N_{\text{quad}}\}.$$

2: Center the process

$$u_c(\mathbf{x}_m, \boldsymbol{\xi}^k) = U(\mathbf{x}_m, \boldsymbol{\xi}^k) - \bar{U}_m, \quad k \in \{1, \dots, N\}, m \in \{1, \dots, N_{\text{quad}}\}.$$

3: Form the covariance matrix

$$K_{lm} = \frac{1}{N-1} \sum_{k=1}^N u_c(\mathbf{x}_l, \boldsymbol{\xi}^k) u_c(\mathbf{x}_m, \boldsymbol{\xi}^k), \quad l, m \in \{1, \dots, N_{\text{quad}}\}.$$

4: Let  $\mathbf{W} = \text{diag}(w_1, w_2, \dots, w_{N_{\text{quad}}})$  and solve the eigenvalue problem

$$\mathbf{W}^{1/2} \mathbf{K} \mathbf{W}^{1/2} \mathbf{v}_i = \lambda_i \mathbf{v}_i, \quad i \in \{1, \dots, N_{\text{quad}}\}.$$

5: Compute  $\mathbf{e}_i = \mathbf{W}^{-1/2} \mathbf{v}_i$ ,  $i \in \{1, \dots, N_{\text{quad}}\}$ .

6: Compute the discretized KL modes,

$$u_i(\boldsymbol{\xi}^k) = \frac{1}{\sqrt{\lambda_i}} \sum_{m=1}^{N_{\text{quad}}} w_m u_c(\mathbf{x}_m, \boldsymbol{\xi}^k) e_i^m, \quad i \in \{1, \dots, N_{kl}\}, k \in \{1, \dots, N\}.$$


---

**Spectral representation of  $p(x, \omega)$ .** In this section, we study the approximation of the PDE solution  $p(x, \omega)$  using truncated KL expansions computed using Algorithm 1. We begin by depicting the correlation function of  $p(x, \omega)$  in Figure 2 (left) approximated via Monte Carlo sampling with  $10^4$  samples; this illustrates the long correlation lengths observed in the solution of the uncertain boundary value problem. Hence, we expect that the eigenvalues of the covariance operator of  $p(x, \omega)$  will exhibit faster decay as compared to eigenvalues of  $C_Z$ . This observation is shown to be the case in Figure 2 (middle) where we compare the (normalized) eigenvalues of the covariance operators for  $p(x, \omega)$  and  $a(x, \omega)$ . This suggests that  $p(x, \omega)$  can be approximated well with a truncated KL expansion with a small number

of terms. Hence, we consider the KL expansion

$$p(x, \omega) = \bar{p}(x) + \sum_{j=1}^{\infty} \sqrt{\mu_j} p_j(\omega) v_j(x). \quad (12)$$

of  $p(x, \omega)$ , where  $\mu_j, v_j$  are the eigenpairs of covariance operator of  $p$ , computed numerically,  $p_j$  are given by

$$p_j(\omega) = \frac{1}{\sqrt{\mu_j}} \int_D (p(x, \omega) - \bar{p}(x)) v_j(x) dx, \quad j = 1, 2, \dots,$$

and  $\bar{p}(x)$  is the mean of  $p(x, \omega)$ . One way to quantify the impact of truncating the KL expansion of  $p(x, \omega)$  on its approximation properties is to study the pointwise variance  $\text{Var}[p(x, \omega)]$  with

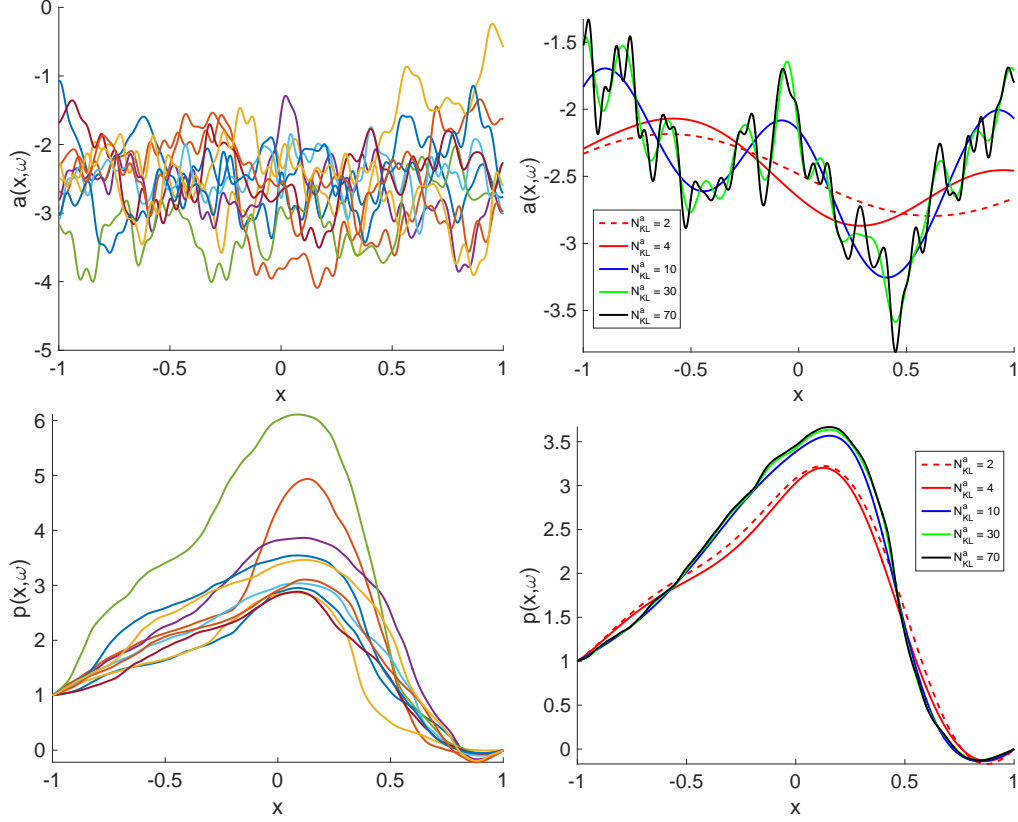


**FIGURE 1.** Top row: Several realizations of the log-coefficient field with  $N_{\text{KL}}^a = 70$  (left); and a fixed realization of the log-coefficient field as we increase  $N_{\text{KL}}^a$  (right). Bottom row: Solutions of the problem (6) corresponding to the realizations of the log-permeability field plotted in the top-left image (left), and a fixed realization of  $p(x, \omega)$  as we increase  $N_{\text{KL}}^a$  (right).

different truncation levels. It is straightforward to see

$$\text{Var} \left[ \sum_{j=1}^{N_{kl}^p} \sqrt{\mu_j} p_j(\omega) v_j(x) \right] = \sum_{j=1}^{N_{kl}^p} \mu_j v_j(x)^2.$$

In Figure 2 (right), we see that it is possible to approximate the pointwise variance of  $p(x, \omega)$  well with a small  $N_{kl}^p$ .

These numerical experiments lead to the following conclusions:

- It is possible to reduce parameter dimension by focusing on KL terms of the parameter that the PDE solution operator is most sensitive to.
- It is possible to reduce output dimension by focusing on the dominant KL terms of the output.

Based on these observation, we next examine parameter and output dimension reduction. In Figure 3 we depict typical realizations of  $p(x, \omega)$ , as the parameter and output dimension is sys-

tematically reduced. These results indicate that simultaneous parameter and output dimension reduction is possible.

## APPLICATION TO BIOTRANSPORT IN TUMORS

**Governing equations and numerical setup.** In this section, we study the pressure field in a tumor when a single needle injection occurs at the tumor center. A 2D model in a polar coordinate system is used to analyze the flow field. Consider the mass conservation law and Darcy's law for steady incompressible flows in a 2D domain,  $D = \{(r, \theta) : R_{\text{needle}} < r < R_{\text{tumor}}, 0 < \theta < 2\pi\}$ ,

$$\frac{\partial}{\partial r} \left( \frac{\kappa r}{\mu} \frac{\partial p}{\partial r} \right) + \frac{1}{r} \frac{\partial}{\partial \theta} \left( \frac{\kappa}{\mu} \frac{\partial p}{\partial \theta} \right) = 0. \quad (13)$$

Here  $p$  is the pressure,  $\kappa$  is the permeability,  $\mu$  is the fluid dynamic viscosity,  $r$  is the radial distance from a fixed origin,  $\theta$  is the polar angle,  $R_{\text{tumor}}$  is the radius of the tumor, and  $R_{\text{needle}}$  is the radius of the needle used to inject nanofluid into the tumor.

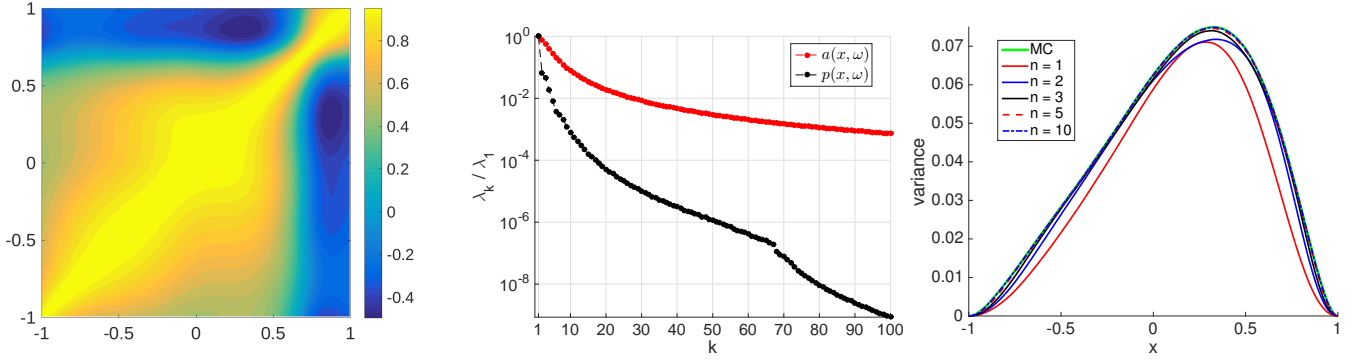


**FIGURE 2.** Left: Correlation function; middle: decay of the spectrum of  $a(x, \omega)$  (red) versus that of the solution  $p(x, \omega)$  (black); we report the first 100 normalized eigenvalues with correlation length of 1/4 for the log-parameter field  $a(x, \omega)$ . Right: pointwise variance of  $p(x, \omega)$ , computed using KL expansion of varying truncation levels, against pointwise variance computed using 10,000 Monte Carlo samples.

The boundary conditions for the pressure equation are specified as follows:

$$\begin{cases} p = 0, & r = R_{\text{tumor}}, \\ \frac{\partial p}{\partial r} = \frac{-Q\mu}{2\pi R_{\text{needle}}\kappa}, & r = R_{\text{needle}}. \end{cases} \quad (14)$$

Herein,  $Q$  is the volume flow rate per unit length. Periodic boundary conditions are enforced in the  $\theta$  direction. In this study,  $R_{\text{needle}}$  and  $R_{\text{tumor}}$  are set to 0.25 mm and 5 mm, respectively. Here  $Q$  is 0.2 mm<sup>2</sup>/min, and  $\mu$  is  $8.9 \times 10^{-4}$  Pa · s.

**Uncertainties in permeability field.** As before let  $(\Omega, \mathcal{F}, P)$  be a probability space. Following [4], the permeability  $\kappa$  is modeled by a log-Gaussian random field, and its mode is set to 0.5 md, where md stands for millidarcy. We assume that the log-permeability,  $a(\mathbf{x}, \omega) = \log(\kappa(\mathbf{x}, \omega))$ , is given by

$$a(\mathbf{x}, \omega) = a_0(\mathbf{x}) + \sigma_a Z(\mathbf{x}, \omega), \quad \mathbf{x} \in D, \omega \in \Omega.$$

Here  $a_0$  is the pointwise mean of the process,  $\sigma_a^2$  is the pointwise variance, and  $Z$  is a centered Gaussian process with unit pointwise variance for every  $\mathbf{x} \in D$ . Herein,  $\sigma_a^2$  is set to 0.25, and  $a_0$  is calculated from the definition of the mode of  $\kappa$  as  $a_0 = \ln(0.5) + \sigma_a^2$ . The covariance function of  $Z$  is expressed as  $c_Z(\mathbf{x}, \mathbf{y}) = \exp\{-\frac{1}{\ell}\|\mathbf{x} - \mathbf{y}\|_2\}$ ,  $\mathbf{x}, \mathbf{y} \in D$ , where  $\ell > 0$  is the correlation length. The log-permeability field can be expressed with a truncated KL expansion:

$$a(\mathbf{x}, \omega) \approx a_0(\mathbf{x}) + \sigma_a \sum_{k=1}^{N_{kl}^a} \sqrt{\lambda_k} \xi_k(\omega) e_k(\mathbf{x}), \quad (15)$$

where  $\lambda_k$  and  $e_k$  are eigenpairs of the covariance operator of the

process  $Z$ . As before, due to Gaussianity of the process,  $\xi_k$  are independent standard normal random variables.

Whereas the governing equation is more complex than the previously considered 1D elliptic problem, it is still an elliptic PDE and hence we observe similar behavior in terms of potential for dimension reduction. Two sets of realizations of the permeability field and the corresponding pressure field, when a small correlation length of  $\ell = 0.5$  mm is used for the log-permeability field, are presented in Figure 4. We observe that although there exist large fluctuations in the permeability field, the fluctuations in the pressure field are mild. For ease of exposition, we denote the covariance operator of the log-permeability field by  $C_a$  and that of the pressure field by  $C_p$ . The eigenvalues  $\lambda_i(C_p)$  show a far more rapid decay as compared to that of  $C_a$ , as seen in Figure 5 (top left). In Figure 5 (top right), we note that more than 96% of the average variance in  $p$  as computed by  $\sum_{i=1}^k \lambda_i(C_p)$ , is captured the first KL term and adding a few KL terms leads to capturing more than 99% of the power spectrum. The eigenvalues of  $C_p$  are approximated using Algorithm 1, with a Monte Carlo sample of size  $N = 5000$ . Next, we experiment with simultaneously changing  $N_{kl}^a$  and  $N_{kl}^p$ . This is done by considering KL expansions of the log-permeability field with  $N_{kl}^a$  terms, sampling the resulting KL expansion, and computing  $p(\mathbf{x}, \omega)$  by solving the pressure equation for each log-permeability field realization. These samples of the PDE solution are then passed to Algorithm 1 to compute the KL expansion of the pressure field. In Figure 5 (bottom left), we show  $\lambda_k(C_p)$ ,  $k = 1, \dots, 50$ , corresponding to  $N_{kl}^a \in \{32, 75, 150, 300, 600\}$ . We note that even with  $N_{kl}^a = 32$ , we can approximate the first 10 eigenvalues of  $C_p$ , which carry most of the power spectrum, reasonably well. Finally, in Figure 5 (bottom right), we show the approximations to average variance of  $p(\mathbf{x}, \omega)$ , computed by  $\sum_{k=1}^{N_{kl}^p} \lambda_k(C_p)$ , as  $N_{kl}^a$  and  $N_{kl}^p$  change. Again, we see that the average variance can be approximated with reasonable accuracy with small  $N_{kl}^a$  and  $N_{kl}^p$ .

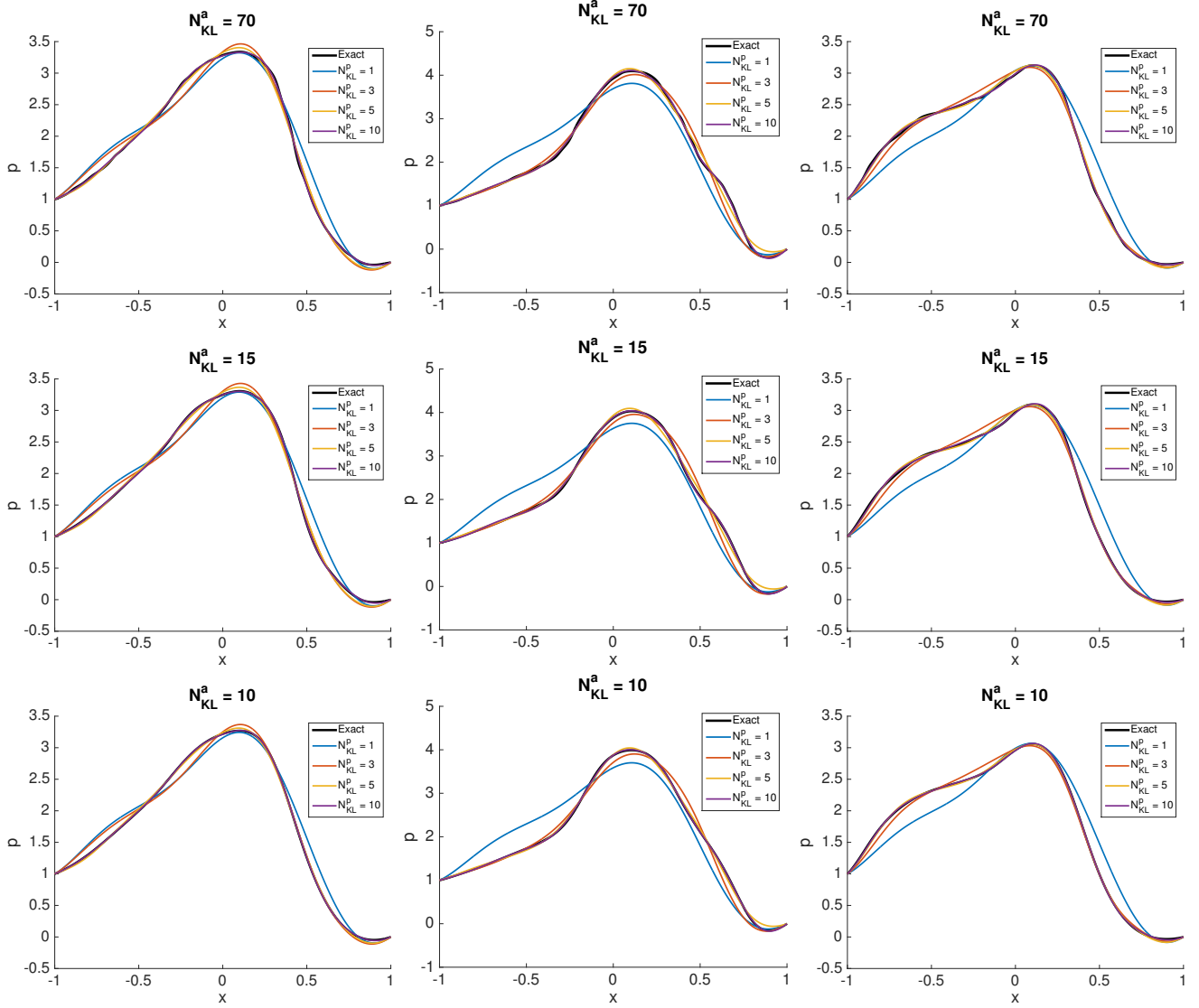


**FIGURE 3.** Realizations of  $p(\mathbf{x}, \omega)$  and the corresponding truncated KL expansions of  $p$ ; each row corresponds to approximations computed with different truncation levels for the parameter, as indicated by  $N_{KL}^a$  in figure titles.

## CONCLUSIONS

We have studied the input parameter and output dimension reduction of elliptic PDEs, with random field input parameters, via the truncated KL expansion technique. In this study, the covariance function of the stochastic process defining the input parameter field is given, and that of the random output is constructed via Monte Carlo sampling. From numerical experiments with both 1D and 2D elliptic PDEs, we observe that when the correlation length is small, very high-dimensional representation is needed to fully resolve the variations in the input field. However, the elliptic operator is not sensitive to high-order KL terms.

As a result, the solution of the elliptic PDE only shows strong dependence to the low-order KL terms of the random input field; moreover, the eigenvalues of the solution covariance operator decay very fast. This enables a low-rank representation of the PDE solution in a low-dimensional input parameter space. We then apply these dimension reduction methods in modeling the bio-transport process in tumors with uncertain material properties, and demonstrate that the pressure field can be approximated with a low-dimensional representation even for random permeability fields with small correlation lengths.

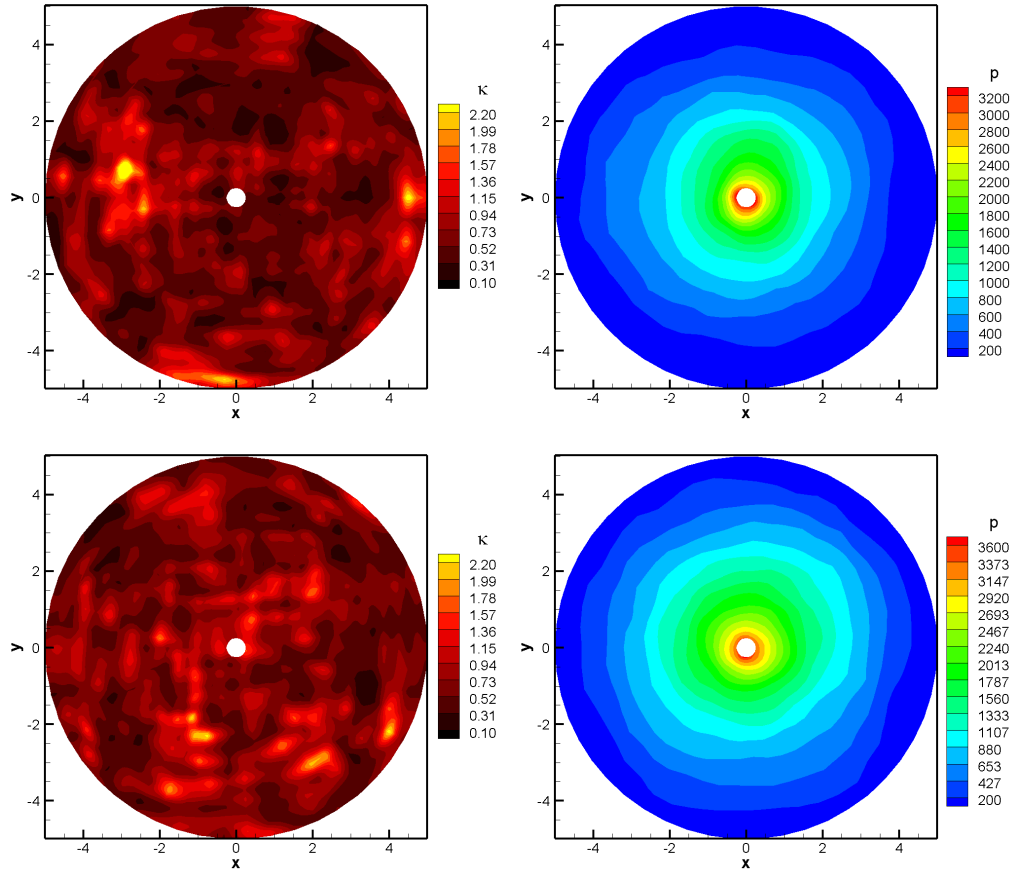


**FIGURE 4.** Two sets of realizations of the permeability field (left) and the corresponding pressure field (right). The correlation length  $\ell$  is 0.5 mm.

## REFERENCES

- [1] Salloum, M., Ma, R., Weeks, D., and Zhu, L., 2008. “Controlling nanoparticle delivery in magnetic nanoparticle hyperthermia for cancer treatment: experimental study in agarose gel”. *Int. J. Hyperthermia*, **24**, pp. 337–345.
- [2] Debbage, P., 2009. “Targeted drugs and nanomedicine: present and future”. *Current Pharmaceutical Design*, **15**, pp. 153–72.
- [3] Swartz, M. A., and Fleury, M. E., 2007. “Interstitial flow and its effects in soft tissues”. *Annu. Rev. Biomed. Eng.*, **9**, pp. 229–56.
- [4] Alexanderian, A., Zhu, L., Salloum, M., Ma, R., and Yu, M., 2017. “Investigation of biotransport in a tumor with uncertain material properties using a non-intrusive spectral uncertainty quantification method”. *Journal of Biomechanical Engineering*, **139**(9), p. 091006.
- [5] Loeve, M., 1977. *Probability theory I*, Vol. 45 of *Graduate Texts in Mathematics*. New York, Heidelberg, Berlin: Springer-Verlag.
- [6] Ghanem, R., 1998. “Probabilistic characterization of transport in heterogeneous media”. *Computer Methods in Applied Mechanics and Engineering*, **158**(3), pp. 199 – 220.
- [7] Le Maître, O. P., Reagan, M. T., Najm, H. N., Ghanem, R. G., and Knio, O. M., 2002. “A stochastic projection method for fluid flow: Ii. random process”. *Journal of computational Physics*, **181**(1), pp. 9–44.
- [8] Xiu, D., and Karniadakis, G. E., 2003. “Modeling uncertainty in flow simulations via generalized polynomial chaos”. *Journal of Computational Physics*, **187**(1), pp. 137 – 167.
- [9] Le Maître, O., Knio, O., Najm, H., and Ghanem, R., 2004. “Uncertainty propagation using wiener–haar expansions”. *Journal of computational Physics*, **197**(1), pp. 28–57.
- [10] Babuška, I., Nobile, F., and Tempone, R., 2007. “A stochastic collocation method for elliptic partial differential equations with random input data”. *SIAM Journal on Numerical Analysis*, **45**(3), pp. 1005–1034.
- [11] Doostan, A., Ghanem, R. G., and Red-Horse, J., 2007. “Stochastic model reduction for chaos representations”. *Computer Methods in Applied Mechanics and Engineering*,

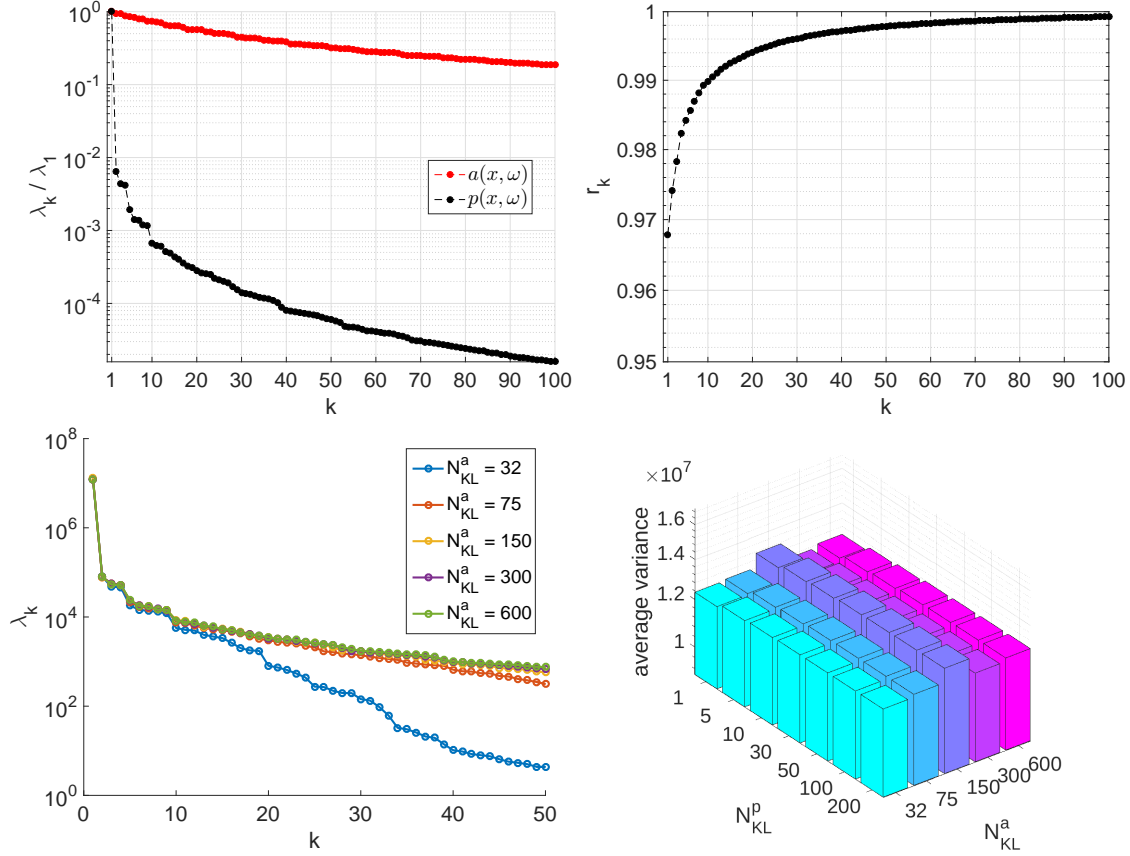


**FIGURE 5.** Top: spectrum of the PDE solution vs spectrum of the uncertain parameter (left); the ratio  $r_k = \sum_{i=1}^k \lambda_i / \sum_{i=1}^N \lambda_i$ , with  $N = 200$ , showing saturation of average variance for model output (right). Bottom: the first 50 eigenvalues of covariance operator for  $p(\mathbf{x}, \boldsymbol{\xi}(\omega))$ , as we increase  $N_{kl}^a$  (left); the average variance of  $p(\mathbf{x}, \boldsymbol{\xi}(\omega))$  as we increase  $N_{kl}^a$  and  $N_{kl}^p$  (right).

*196*(37-40), pp. 3951–3966.

[12] Saad, G., and Ghanem, R., 2009. “Characterization of reservoir simulation models using a polynomial chaos-based ensemble kalman filter”. *Water Resources Research*, **45**(4).

[13] Matthies, H. G., and Keese, A., 2005. “Galerkin methods for linear and nonlinear elliptic stochastic partial differential equations”. *Computer methods in applied mechanics and engineering*, **194**(12-16), pp. 1295–1331.

[14] Graham, I. G., Kuo, F. Y., Nichols, J. A., Scheichl, R., Schwab, C., and Sloan, I. H., 2015. “Quasi-monte carlo finite element methods for elliptic pdes with lognormal random coefficients”. *Numerische Mathematik*, **131**(2), pp. 329–368.

[15] Elman, H., 2017. “Solution algorithms for stochastic galerkin discretizations of differential equations with random data”. *Handbook of Uncertainty Quantification*, pp. 1–16.

[16] Williams, D., 1991. *Probability with martingales*. Cambridge Mathematical Textbooks. Cambridge University Press, Cambridge.

[17] Ghanem, R. G., and Spanos, P. D., 1991. *Stochastic finite elements: a spectral approach*. Springer-Verlag New York, Inc., New York, NY, USA.

[18] Le Maitre, O. P., and Knio, O. M., 2010. *Spectral Methods for Uncertainty Quantification With Applications to Computational Fluid Dynamics*. Scientific Computation. Springer.

[19] Smith, R. C., 2013. *Uncertainty Quantification: Theory, Implementation, and Applications*, Vol. 12. SIAM.

[20] Kress, R., 2014. *Linear integral equations*, third ed., Vol. 82 of *Applied Mathematical Sciences*. Springer, New York.

[21] Betz, W., Papaioannou, I., and Straub, D., 2014. “Numerical methods for the discretization of random fields by means of the karhunen-loève expansion”. *Computer Methods in Applied Mechanics and Engineering*, **271**, pp. 109–129.